Spin Fluctuations from Hertz to Terahertz on a Triangular Lattice

Yusuke Nambu,[1,2,*] Jason S. Gardner,[3,4] Douglas E. MacLaughlin,[5] Chris Stock,[6] Hitoshi Endo,[7,†] Seth Jonas,[8] Taku J. Sato,[1] Satoru Nakatsuji,[9,10] and Collin Broholm[8,3]

[1]*Institute of Multidisciplinary Research for Advanced Materials, Tohoku University, Sendai, Miyagi 980-8577, Japan*
[2]*Neutron Science Laboratory, Institute for Solid State Physics, University of Tokyo, Tokai, Ibaraki 319-1106, Japan*
[3]*NIST Center for Neutron Research, National Institute of Standards and Technology, Gaithersburg, Maryland 20899, USA*
[4]*National Synchrotron Radiation Research Center, Neutron Group, Hsinchu 30077, Taiwan*
[5]*Department of Physics and Astronomy, University of California, Riverside, California 92521, USA*
[6]*School of Physics and Astronomy and Centre for Science at Extreme Conditions, University of Edinburgh, Edinburgh EH9 3FD, United Kingdom*
[7]*Quantum Beam Science Directorate, Japan Atomic Energy Agency, Tokai, Ibaraki 319-1195, Japan*
[8]*Institute for Quantum Matter and Department of Physics and Astronomy, Johns Hopkins University, Baltimore, Maryland 21218, USA*
[9]*Institute for Solid State Physics, University of Tokyo, Kashiwa, Chiba 277-8581, Japan*
[10]*PRESTO, Japan Science and Technology Agency, Saitama 332-0012, Japan*
(Received 4 September 2014; published 15 September 2015)

The temporal magnetic correlations of the triangular-lattice antiferromagnet $NiGa_2S_4$ are examined through 13 decades ($10^{-13} - 1$ sec) using ultrahigh-resolution inelastic neutron scattering, muon spin relaxation, and ac and nonlinear susceptibility measurements. Unlike the short-ranged *spatial* correlations, the temperature dependence of the *temporal* correlations show distinct anomalies. The spin fluctuation rate decreases precipitously upon cooling towards $T^* = 8.5$ K, but fluctuations on the microsecond time scale then persist in an anomalous dynamical regime for $4\text{ K} < T \leq T^*$. As this time scale exceeds that of single-site dynamics by 6 orders of magnitude, these fluctuations bear evidence of emergent degrees of freedom within the short-range correlated incommensurate state of $NiGa_2S_4$.

DOI: 10.1103/PhysRevLett.115.127202 PACS numbers: 75.40.Gb, 75.30.Cr, 76.75.+i, 78.70.Nx

The two-dimensional triangular lattice plays a prominent role in the field of frustrated magnetism. While it now seems clear that the conventional triangular-lattice antiferromagnet has long-range noncollinear 120° Néel order irrespective of the spin quantum number S [1–3], experiments on materials with generalized longer-range interactions, spin-orbit interactions, as well as lattice distortions point to a rich variety of phases in the vicinity of the Néel phase [4,5]. In the quantum limit ($S = 1/2$) first considered by Anderson [6], experiments on organic materials suggest a gapless spin liquid with a spinon Fermi surface may exist near the metal insulator transition [7]. Recent exact diagonalization showed such quantum spin-liquid states can be stabilized by the presence of randomness in the nearest-neighbor interactions [8]. Deep in the insulating limit, neutron scattering experiments suggest conventional spin waves may be supplemented or replaced by a spinon-like continuum even when long-range order is present [9].

For larger spin quantum numbers, theoretical [10] and experimental [11] work points to complex slow spin dynamics that is still poorly understood. Here we focus on such dynamics in the $S = 1$ triangular-lattice antiferromagnet $NiGa_2S_4$ [12,13], which is distinguished by a 2D incommensurate critical wave vector and the potential for spin-nematic interactions [14,15]. Using high-energy-resolution inelastic neutron scattering, neutron spin echo, muon spin relaxation (μSR), and ac magnetometry, we provide evidence for emergent MHz spin dynamics over a wide range of temperatures. We argue such slow spin dynamics is associated with emergent topologically protected degrees of freedom inherent to incommensurate magnetism on the triangular lattice.

Polycrystalline samples of $NiGa_2S_4$ were synthesized by solid-state reaction described elsewhere [16]. Elastic-channel data were taken on the GPTAS and HER triple-axis spectrometers at the JRR-3 research reactor. The backscattering data were taken on the high flux backscattering instrument at the NIST Center for Neutron Research (NCNR) [17]. Neutron spin-echo experiments were performed on the NG5-NSE at NCNR and iNSE spectrometers at the JRR-3; ac susceptibility and nonlinear susceptibilities were measured using a commercial superconducting quantum interference device magnetometer. Detailed descriptions of experiments, analysis of μSR data, and discussion can be found in the Supplemental Material [18].

$NiGa_2S_4$ consists of neutral insulating layers held together by the van der Waals force [Fig. 1(a)]. This curtails electron hopping between layers and leads to a strongly two-dimensional magnet where spin correlations do not extend beyond nearest-neighbor planes [17]. Indeed, a study of the effects of nonmagnetic impurities indicates that quantum collective phenomena in $NiGa_2S_4$ are controlled by intraplane interactions [30]. Within a layer, nickel ions with $S = 1$ reside on an equilateral triangular lattice. $NiGa_2S_4$ is, thus, a rare realization of a highly two-dimensional quantum antiferromagnet. Upholding expectations of anomalous magnetism, the material does not exhibit conventional magnetic order down to temperature $T = 50$ mK. Neutron scattering reveals incommensurate spin correlations with an in-plane correlation length ξ that gradually increases with cooling but tends to 2.6 nm (seven lattice spacings) without a thermal anomaly [Fig. 1(a)].

In sharp contrast, *temporal* correlations feature clear thermal anomalies. Figure 1(b) shows the temperature dependence of the characteristic spin relaxation time τ in $NiGa_2S_4$ and is the central result of this work. Unlike normal magnets, $NiGa_2S_4$ possesses an intermediate temperature regime with spin dynamics on time scales 6 orders of magnitude greater than the time scale set by the exchange constant J. Multiple experimental techniques underlie these data as described in the following. Gallium nuclear quadrupole resonance (NQR) experiments [27] and μSR measurements [28,29] reveal critical slowing-down of Ni-spin fluctuations between the Weiss temperature $|\theta_W| = 80$ K and a characteristic temperature $T^* = 8.5$ K, where nominally elastic diffuse magnetic neutron scattering develops. This is accompanied by a loss of the NQR signal between T^* and 2.5(5) K indicating dynamic nuclear spin relaxation resulting from slow Ni-spin fluctuations [28,29]. μSR provides information for $T < T^*$ where the NQR signal is absent and shows the spin relaxation rate decreases slightly below T^* but remains finite down to 25 mK [29]. These results demonstrate Ni-spin dynamics persists to the lowest temperatures with considerable spectral weight in the MHz frequency range.

Figure 2 shows the temperature dependence of nominally elastic magnetic neutron scattering from polycrystalline $NiGa_2S_4$ as measured with varying spectrometer energy resolutions. The data were obtained on thermal- and cold-neutron triple-axis spectrometers and a backscattering spectrometer [17]. The energy resolution δE sets the minimum spin relaxation time $\tau \sim \hbar/\delta E$ for spin fluctuations that contribute to intensity in the elastic channel. Thus, the gradual appearance of elastic scattering below a δE-dependent crossover temperature signals the development of spin correlations on a time scale beyond $\tau \sim \hbar/\delta E$ (Fig. 2) [31]. The downward shift in onset temperature with tighter energy resolution indicates the time scale for spin fluctuations increases with cooling as presented in Fig. 1(b).

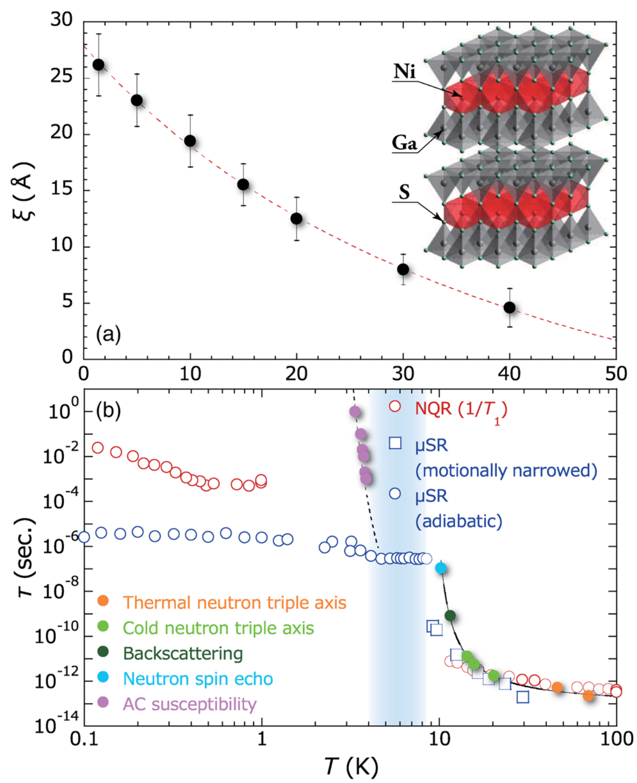

FIG. 1 (color online). Temperature dependence of (a) the spin correlation length ξ and (b) characteristic spin relaxation time τ of $NiGa_2S_4$. The crystal structure of $NiGa_2S_4$ is depicted in the inset to (a). NQR data in (b) are after Ref. [27]. Above and below T^*, the muon spin relaxation rates are in the motionally narrowed ($\propto \tau$) and adiabatic ($\propto 1/\tau$) limits, respectively [28,29] (see the Supplemental Material [18] for details). Vogel-Fulcher behavior from the ac susceptibility measurements is given by the dotted curve. The dashed curve in (a) and the solid curve towards T^* in (b) are guides to the eyes.

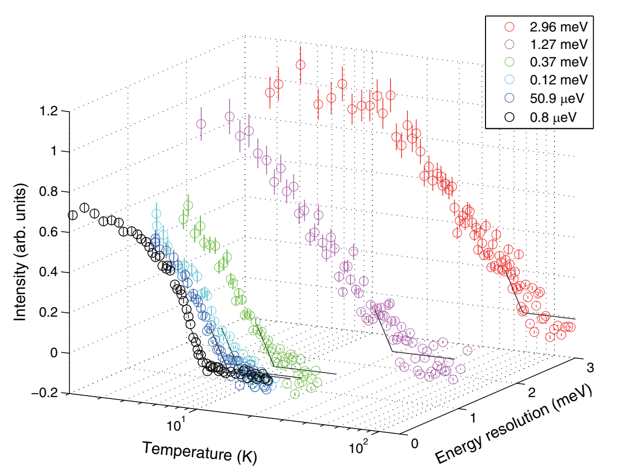

FIG. 2 (color online). Temperature dependence of the elastic-channel data from $NiGa_2S_4$. The nominally elastic signals of the magnetic diffuse scattering from polycrystalline $NiGa_2S_4$ are obtained using thermal-neutron (energy resolution $\delta E = 2.96$, 1.27 meV) and cold-neutron ($\delta E = 0.37$, 0.12 meV, 50.9 μeV) triple-axis spectrometers at the wave vector $Q = 0.58$ Å^{-1} and the backscattering spectrometer ($\delta E = 0.8$ μeV) at $Q = 0.76$ Å^{-1} [17].

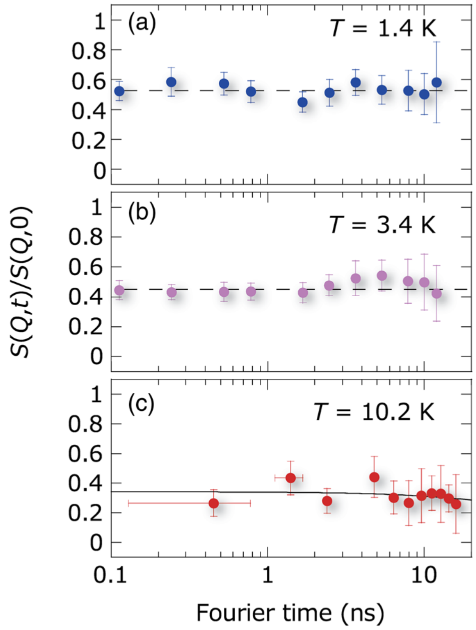

FIG. 3 (color online). Fourier time t dependence of the intermediate scattering function $S(Q,t)/S(Q,0)$ of $NiGa_2S_4$. (a) $T = 1.4$ K data and (b) $T = 3.4$ K data were acquired on the NG5-NSE instrument at NCNR. (c) $T = 10.2$ K data were obtained on the C2-3-1-iNSE instrument at JRR-3. All the data were taken at wave-vector transfer $Q = 0.65$ Å^{-1}. The dashed lines in (a) and (b) give the averages, and an exponential decay fit is shown as the solid line in (c).

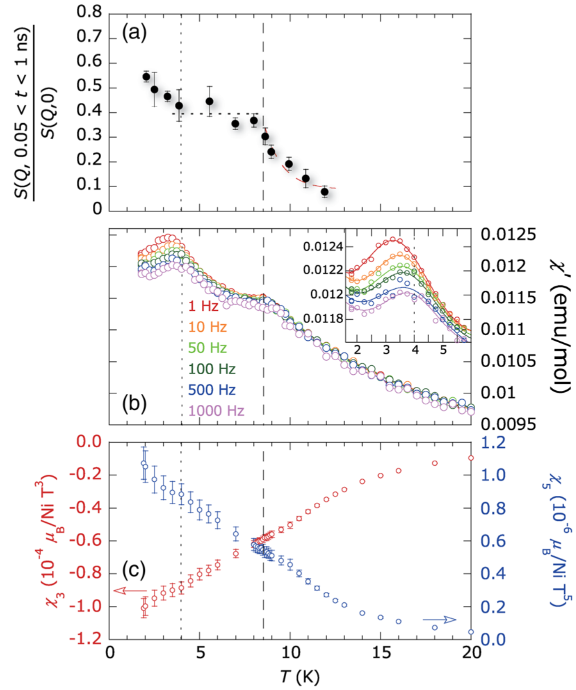

FIG. 4 (color online). Temperature dependence of (a) the averaged intermediate scattering function $S(Q, 0.05 \leq t \leq 1\ \text{ns})/S(Q,0)$, (b) ac, and (c) nonlinear susceptibilities, the coefficient of the third power (left axis) and the fifth power (right axis). The dashed curve and horizontal dotted line in (a) are guides to the eyes. The inset to (b) emphasizes the frequency dependence of χ' at low temperatures. The vertical dashed and dotted lines denote $T^* = 8.5$ K and $T_0 = 4(1)$ K, respectively.

The smallest value of δE is obtained using the neutron spin-echo (NSE) technique. The resulting dependence of the intermediate scattering function (ISF) $S(Q,t)/S(Q,0)$ on Fourier time t is shown in Fig. 3 for three representative temperatures. To estimate the relaxation time τ, the data were fit to a simple exponential decay form, $\exp(-t/\tau)$. For data taken at $T = 10.2$ K [Fig. 3(c)] where a slight reduction in $S(Q,t)/S(Q,0)$ is visible up to $t = 16$ ns, the fit yields $\tau \sim 0.11(5)$ μs with reduced $\chi^2 = 3.971(6)$. A fit to constant ISF leads to $\chi^2 = 4.014(6)$. Figures 3(a) and 3(b) show that below T^*, $S(Q,t)/S(Q,0)$ is constant and does not show any apparent relaxation. Assuming exponential decay, the data place a lower limit of $\tau = 1.3$ μs on the corresponding relaxation time. The fact that $S(Q,t)/S(Q,0) < 1$ for early times indicates fast initial relaxation, and the decrease of $S(Q, t > 0.1\ \text{ns})/S(Q,0)$ with increasing temperature (Fig. 3) indicates a corresponding reduction in the fraction of spins participating in slow relaxation. Given the temperature dependence of the ISF for Fourier time ranging from 0.05 to 1.0 ns (see the Supplemental Material [18]), we interpret the ISF as the volume fraction of spins correlated in accordance with the critical wave vector Q_c and relaxing at times beyond the Fourier time. The temperature dependence of the time-averaged ISF for $0.05 \leq t \leq 1$ ns is given in Fig. 4(a). Reflecting the behavior of τ for $T_0 \leq T \leq T^*$, where $T_0 \sim 4(1)$ K [Fig. 1(b)], there is a temperature regime where the time-averaged ISF is approximately constant possibly due to quantum tunneling. The time-averaged ISF, however, increases upon cooling below T_0, indicating slow dynamics through a larger fraction of the sample, which eventually results in recovery of the NQR signal for $T \leq 2.5(5)$ K [27].

For access to the MHz time scale, we turn to μSR. A description of the method employed to infer a relaxation time from μSR data can be found in the Supplemental Material [18]. Interestingly, the relaxation times from resonance data are considerably shorter than inferred from neutron scattering for $T < 1.5T^*$. This does not, however, represent a discrepancy since the techniques probe different aspects of the spin correlations. In conjunction, the results indicate critical spin-pair correlations probed by neutron scattering at Q_c persist on a longer time scale than the Q-averaged correlations probed by NQR and μSR.

To investigate ultraslow spin dynamics, we use ac susceptibility measurements, which probe the uniform $Q \equiv 0$ response. Figure 4(b) gives the in-phase component χ' as a function of temperature for frequencies from 1 to 1000 Hz. While no significant frequency dependence is observed at the T^* anomaly where the spin fluctuation rate is in the MHz range, frequency dependence is observed for $T \approx 3$ K where the NQR signal is recovered [27]. Below

2.5(5) K, a quasistatic inhomogeneous internal field was inferred from the NQR experiments [27], while μSR is inhomogeneous at all temperatures [28,29]. These observations indicate a wide distribution of spin fluctuation rates, which is corroborated by the distinct time scales inferred from μSR, NQR, and ac susceptibility data [Fig. 1(b)]. That this distribution is strongly Q dependent should be expected given the Q dependence of magnetic neutron scattering and is witnessed by the longer relaxation times for $Q = 0$ ac susceptibility and Q_c neutron scattering data compared to local probes (μSR and NQR). The relatively slow fluctuations seen in NQR could be responsible for the quasistatic component of the μSR signal. Extrapolation of the Vogel-Fulcher curve (see the Supplemental Material [18]) for the ac susceptibility shows that microsecond spin dynamics is present at least down to T_0. While neither the μSR nor NSE data exclude a truly static component, the μSR data indicate significant MHz spin dynamics down to 25 mK [29].

At its freezing temperature, a canonical spin glass is predicted to have diverging third- and fifth-order nonlinear susceptibilities, χ_3 and χ_5 [32]. In search of possible spin-glass-type freezing in $NiGa_2S_4$, nonlinear susceptibility measurements were performed. Figure 4(c) shows the temperature dependence of χ_3 and χ_5. Neither shows divergent behavior at T^* or T_0. The quadratic temperature dependence of the low-temperature magnetic-specific heat C_M [12] in $NiGa_2S_4$ also contrasts with the conventional linear-T behavior known for spin glasses. Similar $C_M \sim T^2$ behavior has been reported for quasi-2D Kagomé-related frustrated magnets of deuteronium jarosite [33] and SCGO [34]. The quasi-two-dimensional antiferromagnetic spin correlations revealed by Q-dependent magnetic neutron scattering [12,17] differ qualitatively from the canonical spin glasses, where *no* Q dependence is anticipated [32].

Despite the structural simplicity and considerable theoretical efforts, no theory is so far able to fully account for the unusual magnetism of $NiGa_2S_4$. In the following, we shall discuss models with potential relevance to the experimental findings. In Monte Carlo simulations, classical Heisenberg spins with nearest-neighbor interactions on the triangular lattice exhibit a precipitous decrease in the spin relaxation rate for $T_v/J \sim 0.28$ [35], which may be compared to $T^*/J = 0.43$ [$J = 20(1)$ K from high-T susceptibility data]. This phenomenon has been associated with topological Z_2-vortex ordering [10]. Slow spin dynamics and a finite correlation length are predicted below T_v [35]. Aspects of this theory are in accordance with our findings of consecutive anomalies in the magnetic susceptibility and C_M and the asymptotic behavior of χ_3 (see the Supplemental Material [18]). However, the correlation length predicted in the low-T regime exceeds that observed in $NiGa_2S_4$ by orders of magnitude.

Lacking in this theory as a model for $NiGa_2S_4$ is the quantum nature of Ni spins and the incommensurate Q_c. The semiclassical description of spin degrees of freedom, thus, cannot account for the impurity-spin size dependence of doped $NiGa_2S_4$ [30,36,37]. Specifically, the low-temperature T^2 asymptotic behavior of C_M is preserved only for integer impurity spins that support a quadrupole moment [14,15]. Indeed, a recent theory achieves slow spin dynamics in a nearest-neighbor model of $NiGa_2S_4$ with impurity spins induced by bond disorder with long-range interactions mediated by an antiferroquadrupolar bulk phase [38].

None of these models, however, considers the incommensurate nature of spin correlations in $NiGa_2S_4$ which are thought to arise from competing ferromagnetic nearest-neighbor and antiferromagnetic third nearest-neighbor interactions [12]. Apart from global rotations, the conventional 120° spin structure on the triangular lattice comes in two flavors distinguished by the scalar chirality of the three spins on a specific triangle. However, the incommensurate structure of $NiGa_2S_4$ has three different wave-vector domains, which are related to each other by a C_3 rotation. Monte Carlo simulations show that C_3 symmetry breaking occurs through a finite-temperature first-order phase transition [39,40]. Based on the inferred exchange interactions, the predicted critical temperature ($0.24J_3 \sim 6$ K) is not far from T^*. The Imry-Ma criterion [41], however, implies this transition does not survive under arbitrary weak random field disorder. T^* may, thus, be the remnant of this first-order transition, and the anomalous MHz dynamics might arise from interfaces between the associated C_3 domains [42].

We have characterized megahertz dynamics in a short-range correlated state finding a temperature-dependent relaxation time that is not reflected in temperature-dependent spatial correlations. A spin state with emergent topological degrees of freedom that form at T^* and freeze at lower T may support decoupling between *spatial* and *temporal* two-point spin correlations. Low-frequency ($\hbar\omega \ll J$) and low-temperature ($k_B T < J$) spin fluctuations as reported here are not uncommon in geometrically frustrated magnets, but they are poorly understood. Owing to its structural simplicity and the availability of high-quality single crystals, $NiGa_2S_4$ presents an excellent opportunity for progress towards understanding slow dynamics in spin systems with short-range correlations.

We are grateful for fruitful discussions with P. Dalmas de Réotier, K. Ishida, H. Kawamura, Y. Maeno, S. Onoda, O. Tchernyshyov, H. Tsunetsugu, J.-J. Wen, and J. D. Zhang. This work was partially supported by Grants-in-Aid for Scientific Research from Japan Society for the Promotion of Science (JSPS) (Grants No. 24740223, No. 26800175, and No. 25707030), and by PRESTO of JST, and by Program for Advancing Strategic International Networks to Accelerate the Circulation of Talented Researchers (Grant No. R2604) from JSPS and Grant-in-Aid for Scientific Research on Innovative Areas (Grants No. 15H05882 and

No. 15H05883) from MEXT. Work at IQM was supported by U.S. Department of Energy, Office of Basic Energy Sciences, Division of Materials Sciences and Engineering under Award No. DE-FG02-08ER46544. Work at NIST was supported in part by the National Science Foundation under Agreement No. DMR-0944772. Work at U. C. Riverside was supported by the U.S. National Science Foundation, Grant No. 0801407.

*Present address: Institute for Materials Research, Tohoku University, Sendai, Miyagi 980-8577, Japan.

†Present address: Neutron Science Laboratory, High Energy Accelerator Research Organization, 203-1 Shirakata, Tokai, Ibaraki 319-1106, Japan and Department of Material Structure Science, The Graduate University for Advanced Studies (SOKENDAI), 203-1 Shirakata, Tokai, Ibaraki 319-1106, Japan.

[1] D. A. Huse and V. Elser, Phys. Rev. Lett. **60**, 2531 (1988).
[2] B. Bernu, C. Lhuillier, and L. Pierre, Phys. Rev. Lett. **69**, 2590 (1992).
[3] L. Capriotti, A. E. Trumper, and S. Sorella, Phys. Rev. Lett. **82**, 3899 (1999).
[4] K. Kanoda and R. Kato, Annu. Rev. Condens. Matter Phys. **2**, 167 (2011).
[5] F. L. Pratt, P. J. Baker, S. J. Blundell, T. Lancaster, S. Ohira-Kawamura, C. Baines, Y. Shimizu, K. Kanoda, I. Watanabe, and G. Saito, Nature (London) **471**, 612 (2011).
[6] P. W. Anderson, Mater. Res. Bull. **8**, 153 (1973).
[7] S. Yamashita, Y. Nakazawa, M. Oguni, Y. Oshima, H. Nojiri, Y. Shimizu, K. Miyagawa, and K. Kanoda, Nat. Phys. **4**, 459 (2008).
[8] K. Watanabe, H. Kawamura, H. Nakano, and T. Sakai, J. Phys. Soc. Jpn. **83**, 034714 (2014).
[9] H. D. Zhou, C. Xu, A. M. Hallas, H. J. Silverstein, C. R. Wiebe, I. Umegaki, J. Q. Yan, T. P. Murphy, J.-H. Park, Y. Qiu, J. R. D. Copley, J. S. Gardner, and Y. Takano, Phys. Rev. Lett. **109**, 267206 (2012).
[10] H. Kawamura and S. Miyashita, J. Phys. Soc. Jpn. **53**, 4138 (1984).
[11] A. Olariu, P. Mendels, F. Bert, B. G. Ueland, P. Schiffer, R. F. Berger, and R. J. Cava, Phys. Rev. Lett. **97**, 167203 (2006).
[12] S. Nakatsuji, Y. Nambu, H. Tonomura, O. Sakai, S. Jonas, C. Broholm, H. Tsunetsugu, Y. Qiu, and Y. Maeno, Science **309**, 1697 (2005).
[13] S. Nakatsuji, Y. Nambu, and S. Onoda, J. Phys. Soc. Jpn. **79**, 011003 (2010).
[14] H. Tsunetsugu and M. Arikawa, J. Phys. Soc. Jpn. **75**, 083701 (2006).
[15] A. Läuchli, F. Mila, and K. Penc, Phys. Rev. Lett. **97**, 087205 (2006).
[16] Y. Nambu, R. T. Macaluso, T. Higo, K. Ishida, and S. Nakatsuji, Phys. Rev. B **79**, 214108 (2009).
[17] C. Stock, S. Jonas, C. Broholm, S. Nakatsuji, Y. Nambu, K. Onuma, Y. Maeno, and J.-H. Chung, Phys. Rev. Lett. **105**, 037402 (2010).
[18] See Supplemental Material at http://link.aps.org/supplemental/10.1103/PhysRevLett.115.127202, which includes Refs. [19–26], for detailed descriptions of experiments.
[19] G. Ehlers, J. S. Gardner, C. H. Booth, M. Daniel, K. C. Kam, A. K. Cheetham, D. Antonio, H. E. Brooks, A. L. Cornelius, S. T. Bramwell, J. Lago, W. Häussler, and N. Rosov, Phys. Rev. B **73**, 174429 (2006).
[20] H. Vogel, Phys. Z. **22**, 645 (1921).
[21] G. S. Fulcher, J. Am. Ceram. Soc. **8**, 339 (1925).
[22] J. L. Tholence, Solid State Commun. **35**, 113 (1980).
[23] J. J. Prejean, J. Phys. (Paris), Colloq. **39**, C6-907 (1978).
[24] J. Dho, W. S. Kim, and N. H. Hur, Phys. Rev. Lett. **89**, 027202 (2002).
[25] H. Bouchiat, J. Phys. (Paris) **47**, 71 (1986).
[26] R. S. Hayano, Y. J. Uemura, J. Imazato, N. Nishida, T. Yamazaki, and R. Kubo, Phys. Rev. B **20**, 850 (1979).
[27] H. Takeya, K. Ishida, K. Kitagawa, Y. Ihara, K. Onuma, Y. Maeno, Y. Nambu, S. Nakatsuji, D. E. MacLaughlin, A. Koda, and R. Kadono, Phys. Rev. B **77**, 054429 (2008).
[28] D. E. MacLaughlin, Y. Nambu, S. Nakatsuji, R. H. Heffner, L. Shu, O. O. Bernal, and K. Ishida, Phys. Rev. B **78**, 220403(R) (2008).
[29] S. Zhao, P. Dalmas de Réotier, A. Yaouanc, D. E. MacLaughlin, J. M. Mackie, O. O. Bernal, Y. Nambu, T. Higo, and S. Nakatsuji, Phys. Rev. B **86**, 064435 (2012).
[30] Y. Nambu, S. Nakatsuji, and Y. Maeno, J. Phys. Soc. Jpn. **75**, 043711 (2006).
[31] A. P. Murani and A. Heidemann, Phys. Rev. Lett. **41**, 1402 (1978).
[32] J. A. Mydosh, *Spin Glasses, an Experimental Introduction* (Taylor & Francis, London, 1993).
[33] A. S. Wills, A. Harrison, S. A. M. Mentink, T. E. Mason, and Z. Tun, Europhys. Lett. **42**, 325 (1998).
[34] A. P. Ramirez, G. P. Espinosa, and A. S. Cooper, Phys. Rev. Lett. **64**, 2070 (1990).
[35] H. Kawamura, A. Yamamoto, and T. Okubo, J. Phys. Soc. Jpn. **79**, 023701 (2010).
[36] Y. Nambu, S. Nakatsuji, Y. Maeno, E. K. Okudzeto, and J. Y. Chan, Phys. Rev. Lett. **101**, 207204 (2008).
[37] Y. Nambu and S. Nakatsuji, J. Phys. Condens. Matter **23**, 164202 (2011).
[38] J. Takano and H. Tsunetsugu, J. Phys. Soc. Jpn. **80**, 094707 (2011).
[39] R. Tamura and N. Kawashima, J. Phys. Soc. Jpn. **77**, 103002 (2008).
[40] E. M. Stoudenmire, S. Trebst, and L. Balents, Phys. Rev. B **79**, 214436 (2009).
[41] T. Nattermann, in *Spin Glasses and Random Fields*, edited by A. P. Young (World Scientific, Singapore, 1997).
[42] Y. Tomita and M. Žukovič, J. Phys. Soc. Jpn. **83**, 083001 (2014).